

NON-PERTURBATIVE BOTTOM PDF AND ITS POSSIBLE IMPACT ON NEW PHYSICS SEARCHES*

ALEKSANDER KUSINA

Laboratoire de Physique Subatomique et de Cosmologie
53 Rue des Martyrs Grenoble, France

(Received April 11, 2016)

Heavy quark parton distribution functions (PDFs) play an important role in several Standard Model and new physics processes. Most PDF analyses rely on the assumption that the charm and bottom PDFs are generated perturbatively by gluon splitting and do not include any non-perturbative degrees of freedom. However, a non-perturbative, intrinsic heavy quark PDFs have been predicted in the literature. We demonstrate that to a very good approximation, the scale-evolution of the intrinsic heavy quark content of the nucleon is governed by non-singlet evolution equations, and use this approximation to model the intrinsic bottom distribution and its impact on parton-parton luminosities at the LHC.

DOI:10.5506/APhysPolB.47.1519

1. Introduction

Heavy quark parton distribution functions (PDFs) play an important role in several Standard Model (SM) and new physics processes at the LHC. In particular, several key processes involve the bottom quark PDF, *e.g.* tW , tH^+ production, associated b plus $W/Z/H$ boson production or Hbb production [1]. In the standard approach employed by almost all global analyses of PDFs, the heavy quark distributions are generated *radiatively*, according to DGLAP evolution equations starting with a perturbatively calculable boundary condition [2, 3] at a scale of the order of the heavy quark mass. In other words, there are no free fit parameters associated with the heavy quark distribution and it is entirely related to the gluon PDF at the scale of the boundary condition. As a consequence, the uncertainties for the heavy quark and gluon distributions are strongly correlated.

* Presented at the Cracow Epiphany Conference on the Physics in LHC Run 2, Kraków, Poland, January 7–9, 2016.

However, a purely perturbative, *extrinsic*, treatment where the heavy quarks are radiatively generated might *not* be adequate; in particular, for the charm quark with a mass $m_c \simeq 1.3$ GeV which is not much bigger than typical hadronic scales but also for the bottom quark with a mass $m_b \simeq 4.5$ GeV. Indeed, there are a number of models that postulate a non-perturbative, *intrinsic*, heavy quark component which is present even for scales Q below the heavy quark mass m . In particular, light-cone models predict a non-perturbative (*intrinsic*) heavy quark component in the proton wave function [4, 5] and similar expectations result from meson cloud models [6, 7]; for a review of different models, see *e.g.* [8]. Predictions of these models motivated people to investigate the possibility of intrinsic charm (IC) in global PDF analyses [9, 10], and gave the first estimate of how big the intrinsic charm could be. Interestingly, the two new global PDF analyses dedicated to IC from CTEQ [11] and Jimenez-Delgado *et al.* [12] set significantly different limits on the allowed IC contribution¹.

While there are at least a few global analyses which allow for an intrinsic charm component in the nucleon [9–12], studies of intrinsic bottom (IB) PDFs have not been performed at all. In this contribution, we summarize a technique, that we introduced in [13], allowing to obtain IB (and IC) PDFs for any generic non-intrinsic PDF set. Our approach exploits the fact that the intrinsic bottom PDF evolves (to an excellent precision) according to a standalone non-singlet evolution equation and evolution of the other partons is essentially not disturbed.

The rest of this paper is organized as follows. In Sec. 2, we demonstrate that the scale-evolution of the intrinsic PDF is governed by a non-singlet evolution equation. We then propose suitable boundary conditions and perform numerical tests of the quality of our approximations. In Sec. 3, we use the IB and IC PDFs to obtain predictions for parton–parton luminosities relevant at the LHC. Finally, in Sec. 4, we summarize our results and present conclusions. More details about this study can be found in [13].

2. Intrinsic heavy quark PDFs

2.1. Evolution equations

In the context of a global analysis of PDFs, the different parton flavors are specified via a boundary condition at the input scale μ_0 which is typically of the order $\mathcal{O}(1 \text{ GeV})$. Solving the DGLAP evolution equations with these boundary conditions allows us to determine the PDFs at higher scales $\mu > \mu_0$. The boundary conditions for the up, down, strange quarks and gluons are not perturbatively calculable and have to be determined from

¹ This is partly because of the very different tolerance criteria which are used to define the range of acceptable fits.

experimental data. From this perspective, it is meaningless to decompose the light quark and gluon PDFs into distinct (extrinsic and intrinsic) components. The situation is different for the heavy charm and bottom quarks where the boundary conditions have been calculated perturbatively. A non-perturbative (intrinsic) heavy quark distribution Q_1 can then be defined at the input scale μ_0 as the difference of the full boundary condition for the heavy quark PDF Q and the perturbatively calculable (extrinsic) boundary condition Q_0

$$Q_1(x, \mu_0) := Q(x, \mu_0) - Q_0(x, \mu_0), \tag{1}$$

where $Q = c$ or $Q = b$. At NLO in the $\overline{\text{MS}}$ scheme, the relation in Eq. (1) gets further simplified if the input scale μ_0 is identified with the heavy quark mass m_Q because $Q_0(x, m_Q) = 0$. In this case, any non-zero boundary condition $Q(x, m_Q) \neq 0$ can be attributed to the intrinsic heavy quark component.

Using the decomposition of Eq. (1), the DGLAP evolution equations governing the scale dependence of PDFs can be written as²

$$\dot{g} = P_{gg} \otimes g + P_{gq} \otimes q + P_{gQ} \otimes Q_0 + \cancel{P_{gQ} \otimes Q_1}, \tag{2}$$

$$\dot{q} = P_{qq} \otimes g + P_{qq} \otimes q + P_{qQ} \otimes Q_0 + \cancel{P_{qQ} \otimes Q_1}, \tag{3}$$

$$\dot{Q}_0 + \dot{Q}_1 = P_{Qg} \otimes g + P_{Qq} \otimes q + P_{QQ} \otimes Q_0 + P_{QQ} \otimes Q_1. \tag{4}$$

Neglecting the crossed out terms which give a tiny contribution to the evolution of the gluon and light-quark distributions, the system of evolution equations can be separated into two independent parts. For the system of gluon, light quarks and extrinsic heavy quark (g, q, Q_0), one recovers the standard evolution equation without an intrinsic heavy quark component. For the intrinsic heavy quark distribution, Q_1 , one finds a standalone non-singlet evolution equation

$$\dot{Q}_1 = P_{QQ} \otimes Q_1. \tag{5}$$

To fully decouple the two evolution equations, we need to allow for a violation of the momentum sum rule. The violation is of the order of the momentum carried by the intrinsic heavy quarks

$$\int_0^1 dx x (Q_1 + \bar{Q}_1) \tag{6}$$

which is known to be very small, especially for the case of bottom quarks.

² Strictly speaking, the decomposition of Q into Q_0 and Q_1 is defined at the input scale where the calculable boundary condition for Q_0 is known. Only due to the approximations in Eqs. (2) and (3), it is possible to entirely decouple Q_0 from Q_1 so that the decomposition becomes meaningful at any scale.

2.2. Boundary condition

The BHPS model [4] predicts the following x -dependence for the intrinsic charm (IC) parton distribution function

$$c_1(x) = \bar{c}_1(x) \propto x^2 [6x(1+x) \ln x + (1-x)(1+10x+x^2)] . \quad (7)$$

However, the normalization and the precise energy scale of this distribution are not specified. In the CTEQ global analyses with intrinsic charm [9, 10], this functional form has been used as a boundary condition at the scale $Q = m_c$, and in this work we do the same.

In the case of intrinsic bottom, we expect that the x -shape of the boundary condition will be very similar to that of intrinsic charm distribution. However, the normalization of IB is expected to be parametrically suppressed by a factor $m_c^2/m_b^2 \simeq 0.1$. Therefore, we propose the following boundary condition for the IB distribution

$$b_1(x, m_c) = \frac{m_c^2}{m_b^2} c_1(x, m_c) . \quad (8)$$

Let us also note that in our approach, it would *not* be a problem to work with asymmetric boundary conditions, $\bar{c}_1(x) \neq c_1(x)$ and $\bar{b}_1(x) \neq b_1(x)$, as predicted, for example, by meson cloud models [14].

2.3. Intrinsic heavy quark PDFs from non-singlet evolution

We have used approximation of Sec. 2.1 and boundary conditions of Eqs. (7) and (8) to produce a set of standalone IC and IB PDFs. QCD parameters, such as the strong coupling or the quark masses were matched with CTEQ6.6 fits [10]; normalization of IC PDF was fixed to the one obtained in CTEQ6.6c0 fit and IB normalization was respectively scaled. Both PDFs were then evolved according to the non-singlet evolution equation (5) and corresponding grids were produced.

In order to test the ideas presented above, we use the CTEQ6.6c series of intrinsic charm fits [10]. The CTEQ6.6c series comprises 4 sets of PDFs including an intrinsic charm component. Two of them, CTEQ6.6c0 and CTEQ6.6c1, employ the BHPS model with 1% and 3.5% IC probability, respectively. This corresponds to the values of 0.01 and 0.035 of the first moment of the charm PDF, $\int dx c(x)$, calculated at the input scale $Q_0 = m_c = 1.3$ GeV. In the rest of this contribution, we will follow the naming convention of the CTEQ6.6c fits in which a given fit is characterized by the value in percentage of the first moment of the charm distribution at the input scale, *e.g.* 1% for CTEQ6.6c0.

In the following, we compare our approximate IC PDFs supplemented with the central CTEQ6.6 fit, which has a radiatively generated charm distribution, with the CTEQ6.6c0 and CTEQ6.6c1 sets where IC has been obtained from global analysis without the approximations of Sec. 2.1. In Fig. 1 (left panels), we present this comparison for 1% IC normalization for two scales $Q^2 = 1.69$ and 10000 GeV^2 . As can be seen in the ratio plot, the difference between the sum $c_0 + c_1$ and the CTEQ6.6c0 charm distribution is tiny at low Q^2 , and smaller than 5% at higher scales. In other words, the IC distribution c_1 evolved according to the decoupled non-singlet evolution equation is in very good agreement with the difference $c - c_0$ representing the IC component in the full global analysis.

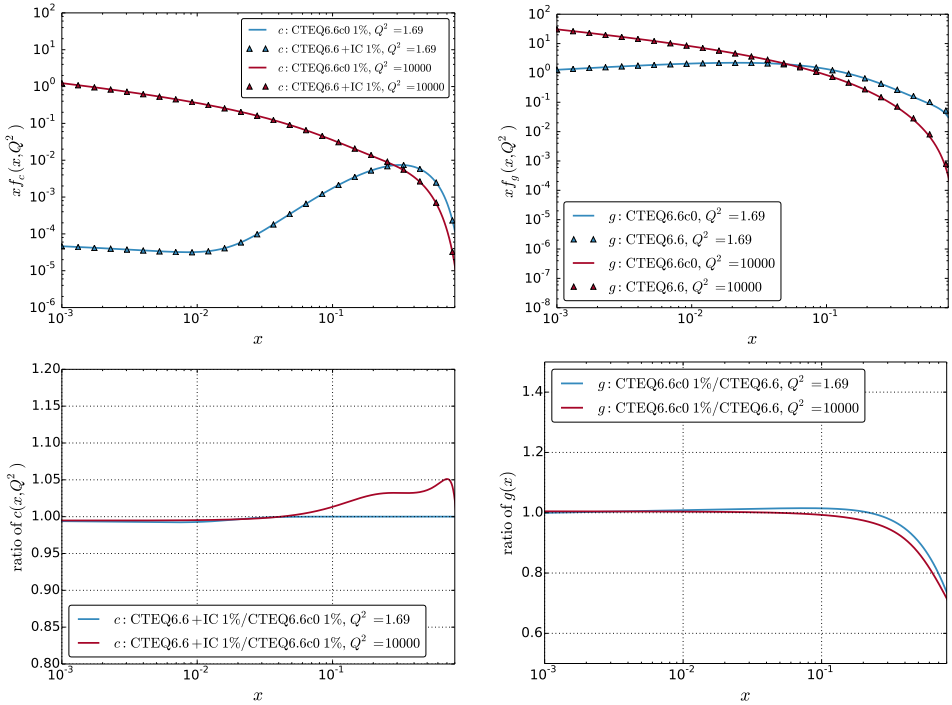


Fig. 1. (Upper left) CTEQ6.6c0 charm distribution function $c(x, Q^2)$ (solid lines) and the sum $c_0(x, Q^2) + c_1(x, Q^2)$ (triangles), where c_0 is the radiatively generated CTEQ6.6 charm distribution and c_1 is the non-singlet evolved IC. (Lower left) Figure shows the ratio of the corresponding curves. (Upper right) Comparison of the CTEQ6.6c0 (solid line) and the CTEQ6.6 (triangles) gluon distributions. (Lower right) shows ratio of the corresponding curves.

Of course, the inclusion of the intrinsic charm distribution will alter the other parton distributions, most notably the gluon PDF. In order to gauge this effect, in right panels of Fig. 1, we compare gluon distribution from the CTEQ6.6c0 analysis with the one from the standard CTEQ6.6 fit. For small x ($x < 0.1$), the gluon PDF is not affected by the presence of a BHPS-like intrinsic charm component which is concentrated at large x . At $x \simeq 0.7$, the CTEQ6.6c0 gluon is suppressed by about 20% with respect to CTEQ6.6, and this is relatively insensitive to the value of Q^2 . We note that at large- x , the gluon distribution is already quite small and the uncertainty of the gluon PDF is sizable (of the order of 40–50% for the CTEQ6.6 set). The difference between the gluon distributions is *slightly* enhanced when evolving from the input scale $Q^2 = 1.69 \text{ GeV}^2$ to the electroweak scale $Q^2 = 10000 \text{ GeV}^2$, but it is still much smaller than the PDF uncertainty. We conclude that for most applications, adding a standalone intrinsic charm distribution to an existing standard global analysis of PDFs is internally consistent and leads to only a small error. Moreover, for the case of intrinsic bottom which is additionally suppressed, the accuracy of the approximation will be even better.

A more detailed numerical validation showing also effects on parton–parton luminosities has been presented in Ref. [13], where we have introduced this method.

3. Possible effects of IC/IB on LHC observables

To provide a generic estimate of possible effects of IC and IB on the LHC observables, we will investigate their impact on parton–parton luminosities at 14 TeV. This allows us to assess the relevance of a non-perturbative heavy quark component for the production of new heavy particles coupling to the SM fermions.

Using the factorization theorem of QCD for hadronic cross sections, one can express the inclusive cross section for the production of a heavy particle H as follows:

$$\sigma_{pp \rightarrow H+X} = \sum_{ij} \int_{\tau}^1 \int_{\tau/x_1}^1 dx_1 dx_2 f_i(x_1, \mu) f_j(x_2, \mu) \hat{\sigma}_{ij \rightarrow H}(\hat{s}), \quad (9)$$

where $\tau = x_1 x_2 = m_H^2/S$, S is the hadronic center-of-mass energy, and $\hat{s} = x_1 x_2 S$ is its partonic counterpart. $f_i(x, \mu)$ denotes the PDF of parton i carrying momentum fraction x inside the proton. Finally, μ is the factorization scale which, in the following, is identified with the partonic center-of-mass energy $\hat{s} = m_H^2$. Equation (9) can be re-written in the form of a convolution of partonic cross sections and parton–parton luminosities,

$$\sigma_{pp \rightarrow H+X} = \sum_{ij} \int_{\tau}^1 d\tau \frac{\mathcal{L}_{ij}}{d\tau} \hat{\sigma}_{ij}(\hat{s}), \tag{10}$$

where

$$\frac{d\mathcal{L}_{ij}}{d\tau}(\tau, \mu) = \frac{1}{1 + \delta_{ij}} \frac{1}{\sqrt{S}} \int_{\tau}^1 \frac{dx}{x} [f_i(x, \mu) f_j(\tau/x, \mu) + f_j(x, \mu) f_i(\tau/x, \mu)]. \tag{11}$$

All the results of this section have been obtained using the CTEQ6.6 PDF set [10] supplemented with our approximate IC and IB PDFs constructed using the procedure presented in Sec. 2.

In Fig. 2 (a), we show different parton–parton luminosities, $d\mathcal{L}_{ij}/d\tau$, for the LHC at 14 TeV (LHC14) as a function of $\sqrt{\tau} = m_H/\sqrt{S}$. We choose the range of $\sqrt{\tau}$ to be [0.02, 0.5] that corresponds to the production of a heavy particle of mass $m_H \in [0.280, 7]$ TeV which is roughly the range of values that will likely be probed at the LHC14. As can be seen, at large $\sqrt{\tau}$, the parton–parton luminosities respect the following ordering: $ug \gg u\bar{u} > gg \gg gc > gb \gg c\bar{c} > b\bar{b}$. Consequently, one can generally conclude that heavy quark initiated subprocesses play a minor role in *most* processes where a heavy state is produced.

One exception would be SM extensions, where the couplings to the first two generations are suppressed or vanish so that the gb or $b\bar{b}$ channels can dominate; typically, this is done in order to avoid experimental constraints from low energy precision observables or flavor changing neutral currents. Of course, unless the couplings to the gb or $b\bar{b}$ channels are enhanced, these scenarios have tiny cross sections and will be difficult to measure at the LHC.

However, if the couplings are enhanced by factors of the quark mass, the hierarchy of the contributions can change dramatically. This can happen when the heavy state has couplings to the Standard Model particles proportional to their masses such as the SM Higgs or the Higgs particles in 2HDM models. For example, in Fig. 2 (a), we show the parton–parton luminosities with no enhancement factors; in Fig. 2 (b), we show the same but with additional factors proportional to the heavy quark mass; the change is dramatic. Taking the quark masses into account, the high τ region now exhibits the following hierarchy: $gg \simeq gb > gc \gg b\bar{b} > c\bar{c} \gg ug \gg u\bar{u}$. In this case, the heavy quark initiated subprocesses could play the dominant role, apart from the gg initiated subprocesses which would contribute via an effective, model-dependent, heavy quark loop-induced ggH coupling.

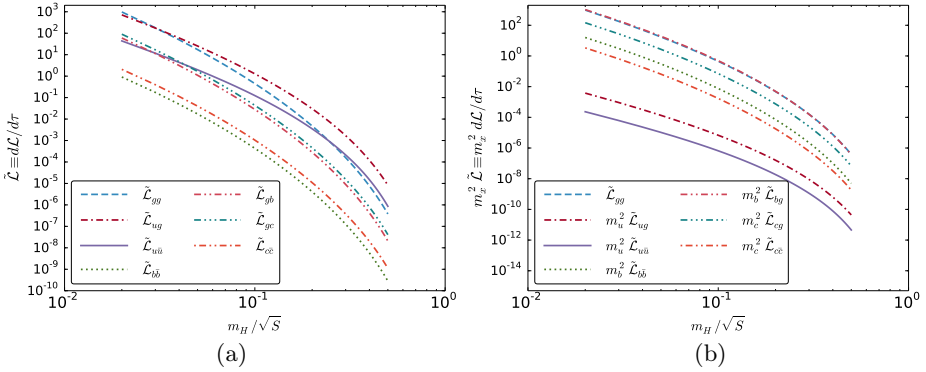


Fig. 2. (a) Different parton–parton luminosities as a function of $\sqrt{\tau} = m_H/\sqrt{S}$ for the LHC14 calculated using CTEQ6.6 PDFs. For large τ , the ordering of the curves is: $ug \gg u\bar{u} > gg \gg gc > gb \gg c\bar{c} > b\bar{b}$. (b) Rescaled parton–parton luminosities ($m_i^2 d\mathcal{L}_{ij}/d\tau$) for the LHC14 calculated using CTEQ6.6 PDFs. For comparison, we also show the un-rescaled gluon–gluon luminosity. For large τ , the ordering of the curves is: $gg \simeq gb > gc \gg b\bar{b} > c\bar{c} \gg ug \gg u\bar{u}$. Note that, by coincidence, the gluon–gluon luminosity, \mathcal{L}_{gg} , agrees at the 10% level with the scaled gb luminosity, $m_b^2 \mathcal{L}_{gb}$, so that the two curves lie on top of each other in (b).

To explore how the presence of IC and IB would affect physics observables with a non-negligible heavy quark initiated subprocesses, in Figs. 3 and 4, we show the ratios of luminosities for charm and bottom with and without an

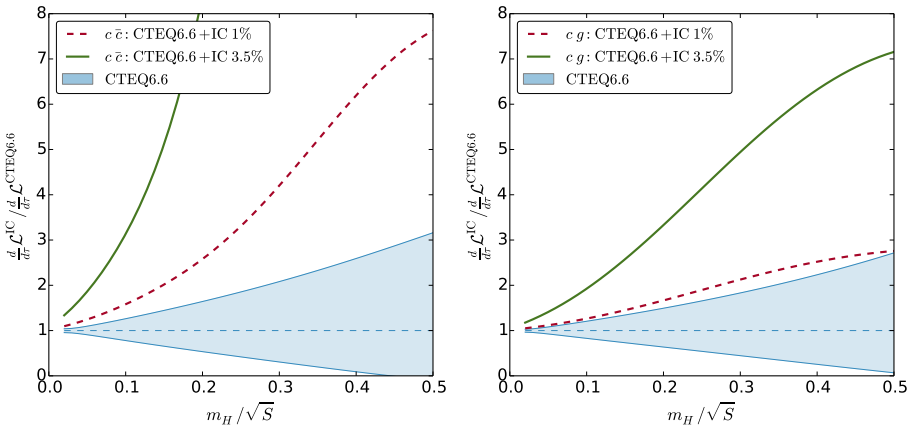


Fig. 3. Ratio of $c\bar{c}$ luminosities (left) and cg luminosities (right) at the LHC14 for charm-quark PDF sets with and without an intrinsic component as a function of $\sqrt{\tau} = m_H/\sqrt{S}$. In addition to the curves with 1% normalization (dashed/red lines), we include the results for the 3.5% normalization (solid/green lines).

intrinsic contribution for 1% and 3.5% normalizations. Furthermore, since there are no experimental constraints on the IB normalization, in Fig. 4, we also include an extreme scenario where we remove the usual m_c^2/m_b^2 factor; thus, the first moment of the IB is 1% at the initial scale m_c .

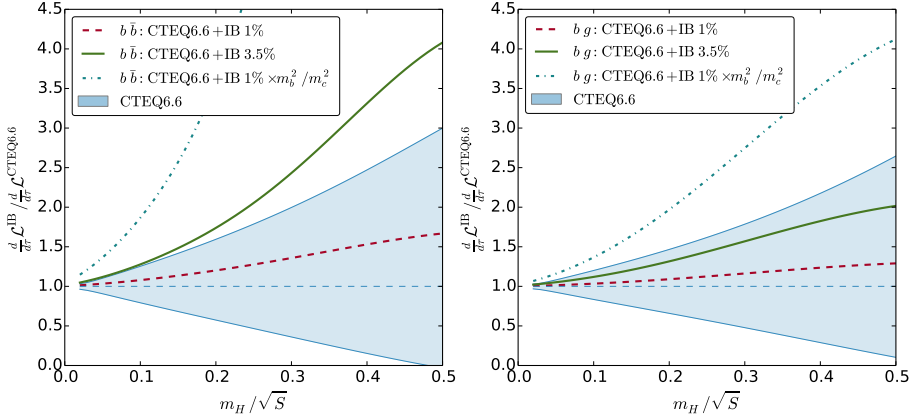


Fig. 4. Ratio of luminosities at the LHC14 for bottom-quark PDF sets with different normalizations of the intrinsic bottom component. The plot has been truncated, and the $b\bar{b}$ luminosity in the extreme scenario reaches about 17 at $\sqrt{\tau} = 0.5$.

For the 1% normalization, the $c\bar{c}$ luminosity ratio grows as large as 7 or 8 for $\sqrt{\tau} = 0.5$, and for a 3.5% normalization, it becomes extremely large and reaches values of up to 50. From these figures, we can clearly see that the effect of the 3.5% IC is substantial and can affect observables sensitive to $c\bar{c}$ and cg channels. As expected, in the case of IB, the effect is smaller but for the $b\bar{b}$ luminosity the IB with 3.5% normalization leads to a curve which lies clearly above the error band of the purely perturbative result. In the extreme scenario (which is not likely but by no means excluded), the IB component has a big effect on both the $b\bar{b}$ and bg channels.

4. Conclusions

We have presented a method to generate a matched IC/IB distributions for any PDF set without the need for a complete global re-analysis. This allows one to easily carry out a consistent analysis including intrinsic heavy quark effects. Because the evolution equation for the intrinsic heavy quarks decouples, we can freely adjust the normalization of the IC/IB PDFs.

For the IB, our approximation holds to a very good precision. For the IC, the error increases (because the IC increases), yet our method is still useful. For an IC normalization of 1–2%, the error is less than the PDF uncertainties at the large- x , where the IC is relevant. For a larger normalization, although

the error may be of the same order as the PDF uncertainties, the IC effects also grow and can be separately distinguished from the case without IC. In any case, the IC/IB represents a non-perturbative systematic effect which should be taken into account.

The method presented here greatly simplifies our ability to search for, and place constraints upon, intrinsic charm and bottom components of the nucleon. This technique will facilitate more precise predictions which may be observed at future facilities such as the Electron Ion Collider (EIC), the Large Hadron–Electron collider (LHeC), or AFTER@LHC.

The PDF sets for intrinsic charm and intrinsic bottom discussed in this analysis (1% IC, 3.5% IC, 1% IB, 3.5% IB) are available from the authors upon request.

REFERENCES

- [1] F. Maltoni, G. Ridolfi, M. Ubiali, *J. High Energy Phys.* **1207**, 022 (2012) [arXiv:1203.6393 [hep-ph]].
- [2] J.C. Collins, W.K. Tung, *Nucl. Phys. B* **278**, 934 (1986).
- [3] M. Buza, Y. Matiounine, J. Smith, W.L. van Neerven, *Eur. Phys. J. C* **1**, 301 (1998) [arXiv:hep-ph/9612398].
- [4] S.J. Brodsky, P. Hoyer, C. Peterson, N. Sakai, *Phys. Lett. B* **93**, 451 (1980).
- [5] S.J. Brodsky, C. Peterson, N. Sakai, *Phys. Rev. D* **23**, 2745 (1981).
- [6] F.S. Navarra, M. Nielsen, C.A.A. Nunes, M. Teixeira, *Phys. Rev. D* **54**, 842 (1996) [arXiv:hep-ph/9504388].
- [7] W. Melnitchouk, A.W. Thomas, *Phys. Lett. B* **414**, 134 (1997) [arXiv:hep-ph/9707387].
- [8] S.J. Brodsky *et al.*, *Adv. High Energy Phys.* **2015**, 231547 (2015) [arXiv:1504.06287 [hep-ph]].
- [9] J. Pumplin, H.L. Lai, W.K. Tung, *Phys. Rev. D* **75**, 054029 (2007) [arXiv:hep-ph/0701220].
- [10] P.M. Nadolsky *et al.*, *Phys. Rev. D* **78**, 013004 (2008) [arXiv:0802.0007 [hep-ph]].
- [11] S. Dulat *et al.*, *Phys. Rev. D* **89**, 073004 (2014) [arXiv:1309.0025 [hep-ph]].
- [12] P. Jimenez-Delgado, T. Hobbs, J. Londergan, W. Melnitchouk, *Phys. Rev. Lett.* **114**, 082002 (2015) [arXiv:1408.1708 [hep-ph]].
- [13] F. Lyonnet *et al.*, *J. High Energy Phys.* **1507**, 141 (2015) [arXiv:1504.05156 [hep-ph]].
- [14] T. Hobbs, J. Londergan, W. Melnitchouk, *Phys. Rev. D* **89**, 074008 (2014) [arXiv:1311.1578 [hep-ph]].